8(d). Hydraulic conditions and mat-related structures in tidal flats and coastal sabkhas

H. Porada, E. Bouougri and J. Ghergut

Introduction

Under specific conditions, cohesive microbial mats may spread out over large areas in the intertidal to lower supratidal zones of tidal flats and coastal sabkhas. In such environments where abundant energy is available from solar irradiation, and CO_2 from the atmosphere, supply of water is the main factor controlling biological activities. Beneficial for initial microbial colonization and establishment of extensive mats are: (i) low hydrodynamic energy; (ii) a fine-grained sandy to silty substrate; (iii) low rate of sediment supply and deposition; (iv) supressed activities of marine mat consumers and burrowers; (v) a steady groundwater flow from the hinterland (see Noffke, 1998b; Gerdes et al., 2000). Examples of extensive microbial mats in such environments have been described from numerous localities in the arid and humid zones, e.g. from the Persian Gulf coast (e.g. Kendall and Skipwith, 1969; Kinsman and Park, 1976), the Mediterranean coast of southern Tunisia (Gerdes et al., 2000; Noffke et al., 2001b), the northeastern coast of Massachusetts (Cameron et al., 1985, with extensive bibliography), and the southern North Sea coast of Germany (e.g. Reineck, 1979; Gerdes et al., 1985c, 2000; Noffke et al., 1996).

In all these cases, the laminated microbial mat is composed of photoautotrophic, filamentous cyanobacteria (e.g. *Microcoleus chthonoplastes*, *Lyngbya aestuarii*) and coccoid cyanobacteria (e.g. *Entophysalis* sp. or *Synechococcus* sp.), which together form the cohesive upper part of the mat, usually between 1-3 mm thick. Underlying are zones with sulphate-reducing bacteria and, in many cases, various anoxygenic phototrophic bacteria (e.g. purple and green sulphur bacteria).

Microbial mats that repeatedly are subaerially exposed, as in the intertidal/lower supratidal zones, tend to develop strongly cohesive, ‘felty’ layers in the upper photic zone, and a ‘leathery’ surface. The internal structure of the ‘felty’ layers is best described as a “condensed fibrillar meshwork” consisting of more or less parallel, “horizontally stretched ensheated filament bundles” (Gerdes et al., 2000, p. 285) which in neighbouring laminae develop perpendicular orientations, leading to a kind of ‘plywood texture’ (Fenchel and Kühl, 2000). A further component in microbial mats is various extracellular polymeric substances (EPS). They are secreted by coccoid cyanobacteria in considerable volume, surround the bacterial cells and sediment grains, and some types may exist in an aggregated gel state of high cohesiveness (Decho, 1994; Stal, 2000). In many modern mats, EPS form a ‘leathery’ surface film which combines high mechanical resistance with very low permeability, inhibiting even the escape of gas rising up from below.

Altogether, the upper part of epibenthic cyanobacterial mats forms a continuous, strongly cohesive zone of low permeability, separating the substratum from the atmosphere and protecting it against water loss. *Vice versa*, the layer of water-saturated sediment below the sealing mat may be described as a ‘confined aquifer’. Therefore, numerical simulations as

In: *Atlas of microbial mat features preserved within the clastic rock record*, Schieber, J., Bose, P.K., Eriksson, P.G., Banerjee, S., Sarkar, S., Altermann, W., and Catuneau, O., (Eds.)J. Schieber et al. (Eds.), Elsevier, p. 258-265. (2007)

applied to respective situations in porous media hydraulics, may be used to compute the hydraulic conditions prevailing in the confined mat substratum.

This paper is focussed on some implications, both biological and physical, arising from upward directed force of hydraulic pressure, locally providing a potential for liquefaction in the mat substratum. It will be argued that hydraulic 'upward pressure' strongly contributes to the survival of mats during dry seasons, that it may trigger localised microbial growth at cracks, and that it may cause local ascent of sediment in the mat substratum. The tidal flats of Bhar Alouane in southern Tunisia (see Fig. 8(d)-1) will serve as an example, but similar conditions are also expected at Sabkhas El Grine, Jellabia, El Mdeina, and Bou Jemel, all in the same region. Modelling of the hydraulic conditions, considering also tidal influences, is presented in Appendix 1.

Some basic considerations about hydraulics

Water completely filling the pore space and flowing downslope through a confined aquifer is under pressure. This 'hydraulic pressure' is a function of the difference in elevation between points where the flow of water enters the confined layer and where it leaves it ('hydraulic heads'). It has the same value along 'equipotential lines' (see Appendix 1), but continuously decreases downslope, in the direction of flow. Hydraulic pressure is thus greatest in the upper part of the slope, where the confining mat begins. It acts against the mat as an 'uplift force' or 'seepage pressure' (e.g. Watson and Burnett, 1995) and may lead to detachment of the mat ('floating failure') and subsequent seepage of groundwater (Fig. 8(d)-2A). Downslope, where the sea temporarily encroaches upon the mat, hydraulic pressure is superimposed by hydrostatic pressure resulting from the load of sea water, increasing in total the 'pore water pressure' in the sediment. From the hydraulic perspective, liquefaction of the sediment may occur when the 'pore water pressure' becomes equal to or exceeds the 'effective stress' induced by the weight of the sediment grains ('excess pressure head'). This may be achieved either if the hydraulic head is raised (e.g. after heavy rains in the hinterland) or if the hydrostatic pressure is increased. The latter is usually the case in the intertidal zone where alternately increasing and decreasing hydrostatic pressures are exerted on the mat surface, according to tidal frequencies.

If evaporation occurs, hydraulic pressure resulting from elevation differences of heads may be complemented by a vertical hydraulic gradient resulting from replacement of the evaporative water-loss near the surface. This 'evaporative pumping' (Hsü and Siegenthaler, 1969) creates an additional uplift force depending on the rate of loss of pore fluids. It will be most effective where microbial mats are not or only scarcely developed and the sediment surface is subaerially exposed, but may also take place beneath mats during low tides to replace water that is lost by evaporation or consumed by the mat organisms.

A naturally occurring example

As a natural example for hydraulic modelling, the tidal flats of Bhar Alouane in southern Tunisia have been selected (Fig. 8(d)-1A). The low-gradient tidal flats extend over several hundred metres inland and are separated from the open sea by a sand barrier which is stabilized by

In: *Atlas of microbial mat features preserved within the clastic rock record,* Schieber, J., Bose, P.K., Eriksson, P.G., Banerjee, S., Sarkar, S., Altermann, W., and Catuneau, O., (Eds.)J. Schieber et al. (Eds.), Elsevier, p. 258-265. (2007)

scattered vegetation. The upper intertidal zone behind the barrier is regularly inundated through narrow tidal channels at high tides. The flats are extensively covered, up to the supratidal zone, by microbial mats which have been described in some detail by Noffke et al. (2001b). Two main mat types have been distinguished by these authors. Firstly, a dark, thick, multi-layered mat dominated by filamentous cyanobacteria, mainly *Microcoleus chthonoplastes* and *Lyngbya aestuarii.* This type is developed in the regularly inundated intertidal zone, locally overlying biolaminites, and in some supratidal ponds. It tends to develop large, polygonally arranged shrinkage cracks which, however, are soon overgrown by new mat layers. Secondly, a brownish, thin, mono-layered mat is found, formed mainly by coccoid cyanobacterial taxa, predominantly *Synechococcus* sp. This mat develops a tough, leathery and very irregular surface, and overlies much of the uppermost interdidal and supratidal zones. Shrinkage cracks are quite rare and usually small in this type of mat. Average annual precipitation in this part of Tunisia is about 175 mm with a large variability, however, between 530 mm/a and 40 mm/a, and with a generally high occurrence of excess rainfall and surface runoff events.

Modelling results and implications

Main results of the hydraulic modelling (see Appendix 1) include: (i) that in coastal sabkhas like Bhar Alouane, considerable upward directed hydraulic pressure (seepage pressure) is built up in the mat substratum; (ii) that over much of the intertidal and supratidal zones, hydraulic pressure attains sufficiently high values to create a potential for liquefaction down to a few centimetres in the sedimentary mat substratum; and (iii) that seepage pressure increases upslope under steady groundwater flow conditions, but decreases in the same direction as the flow of groundwater ceases and tidal hydrodynamics gain in importance. Based on these results the following implications are envisaged:

1.) The results, in general, suggest that groundwater supply to the overlying mat may be sustained even after months of subaerial exposure, as long as traces of groundwater exist in the confined sediment below. This is due to hydraulic ‘upward pressure’, implying upward movement of groundwater. Indeed, it is observed that in the supratidal zone, mats may still contain moisture even after long periods of subaerial exposure. Thus, hydraulic ‘upward pressure' may be a major factor in maintaining microbial mats over dry seasons.
2.) If the sealing mat is interrupted by cracks, however, hydraulic pressure will lead to groundwater discharge at the surface. At such ‘leaking cracks’, availability of water will trigger microbial growth processes in the near-surface population, resulting in overgrowth of the crack opening and the crack margins (Fig. 8(d)-2B, C). This ‘self-healing effect’ keeps the mat intact and resistant against tractional forces acting on the surface (e.g. wind, water currents) and prevents the mat substratum from further groundwater loss.
3.) At narrow ‘leaking cracks’, rapidly initiated microbial growth may spatially not be accomodated in the crack and adjoining mat, leading to bulges and domes along the cracks (Fig. 8(d)-2D - -2F). Such localised ‘mat expansion structures’ (‘petees’ in the original sense of Reineck et al., 1990; see Chapter 6(c)) may be arranged in a polygonal distribution tracing the original shrinkage crack pattern. The shape of the individual structures appears to depend on the microbial species which reacts fastest or most effectively on the sudden availability of water. Thus, bulges (Fig. 8(d)-2F) may indicate that mainly filamentous cyanobacteria were

involved, whereas the domes in Fig. 8(d)-2D, -2E may have resulted from the association between filamentous (*Microcoleus chthonoplastes*) and coccoid cyanobacteria, whereby the filamentous organisms have contributed to the coherent arches, and the coccoids according to their specific way of cell division to irregularities at micro-scales.

4.) Isolated domes, occasionally observed on subaerially exposed mats in supratidal zones (Fig. 8(d)-3A), may also originate from localised water availability. In the supratidal zone of Bou Jemel where gypsum encrusted surface mats of mainly coccoidal bacteria are developed, isolated domes show a close relationship to vertical burrows of rove beetles (*Bledius* sp., G. Gerdes, pers. comm., 2006). It is envisaged that traces of water were seeping out of the burrows thus triggering localised microbial growth and concomitant precipitation of gypsum.

5.) The potential for liquefaction computed for parts of the intertidal/supratidal zones implies that in the mat substratum, grains may momentarily float under effective stress conditions tending to zero, thus loosening the packing in the uppermost millimetres to centimetres of the confined layer. Due to the upward directed force of the hydraulic pressure (possibly complemented by 'evaporative pumping'), an upward movement of grains and water may then be anticipated. This effect may lead to a gradual 'filling from below' of bulges and folds developed in the mat. Even small irregularities of the overlying cohesive mat may be traced in the substratum and become preserved after burial (Fig. 8(d)-3B - 3D). Also shrinkage cracks, if not instantaneously overgrown by new microbial layers, may become filled from below in this way. The process of contemporaneous, hydraulic 'upward pressure'-induced sediment ascent may thus be one of the fundamental mechanisms leading to the preservation of a range of mat-related structures. These may be considered as 'subsurface structures' according to their mode of formation. Sediment ascent and 'filling from below' will be effective mainly in the upper intertidal zone under 'normal' conditions, but may also take place in the supratidal zone after groundwater recharge due to storm-induced flooding or heavy rainfall in the hinterland.

Finally, it has to be stressed that hydraulic conditions and resulting mat-related structures as described in this paper, only apply to the intertidal to supratidal zones of tidal flats/coastal sabkhas, particularly of the arid to subarid climate zone. In other environments, similar structures may evolve from different processes.

In: *Atlas of microbial mat features preserved within the clastic rock record,* Schieber, J., Bose, P.K., Eriksson, P.G., Banerjee, S., Sarkar, S., Altermann, W., and Catuneau, O., (Eds.)J. Schieber et al. (Eds.), Elsevier, p. 258-265. (2007)

Figures

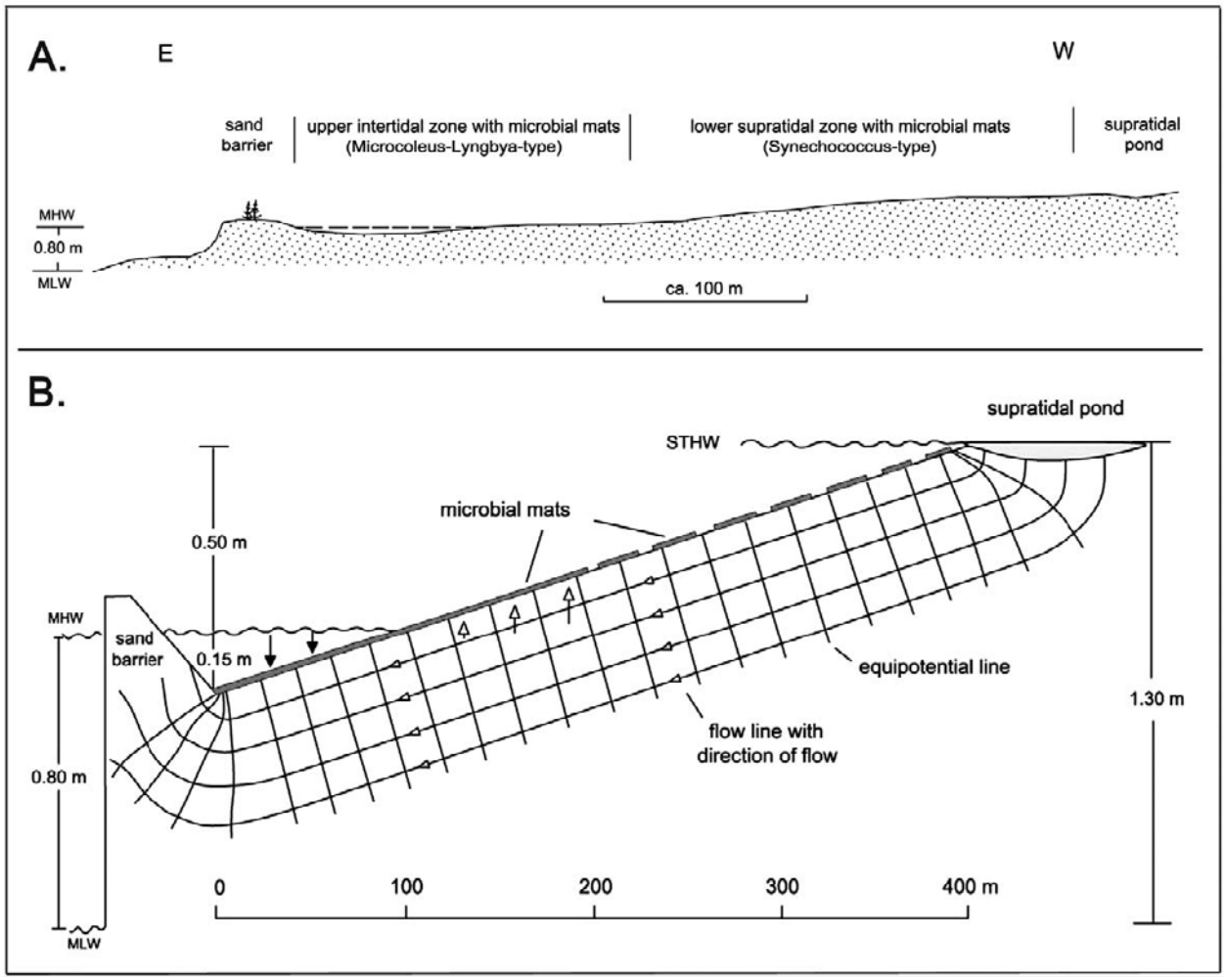

Figure 8(d)-1: Siliciclastic tidal flat hydraulics.
(A) Schematic section across Bhar Alouane tidal flat, Mediterranean coast of southern Tunisia. Tidal range is ca. 0.80 m. Dashed line indicates level and distance up to which the tidal flat is regularly inundated at high tide. MLW = mean low water; MHW = mean high water. Modified after Noffke et al. (2001b). (B) Scenario of a siliciclastic tidal flat protected behind a sand barrier and regularly flooded through tidal channels at high tide. A supratidal pond is assumed to have been filled with water at spring tide or during a storm. Solid arrows indicate hydrostatic pressure; open arrows indicate hydraulic 'upward pressure'. STHW = spring tide high water.

In: *Atlas of microbial mat features preserved within the clastic rock record,* Schieber, J., Bose, P.K., Eriksson, P.G., Banerjee, S., Sarkar, S., Altermann, W., and Catuneau, O., (Eds.)J. Schieber et al. (Eds.), Elsevier, p. 258-265. (2007)

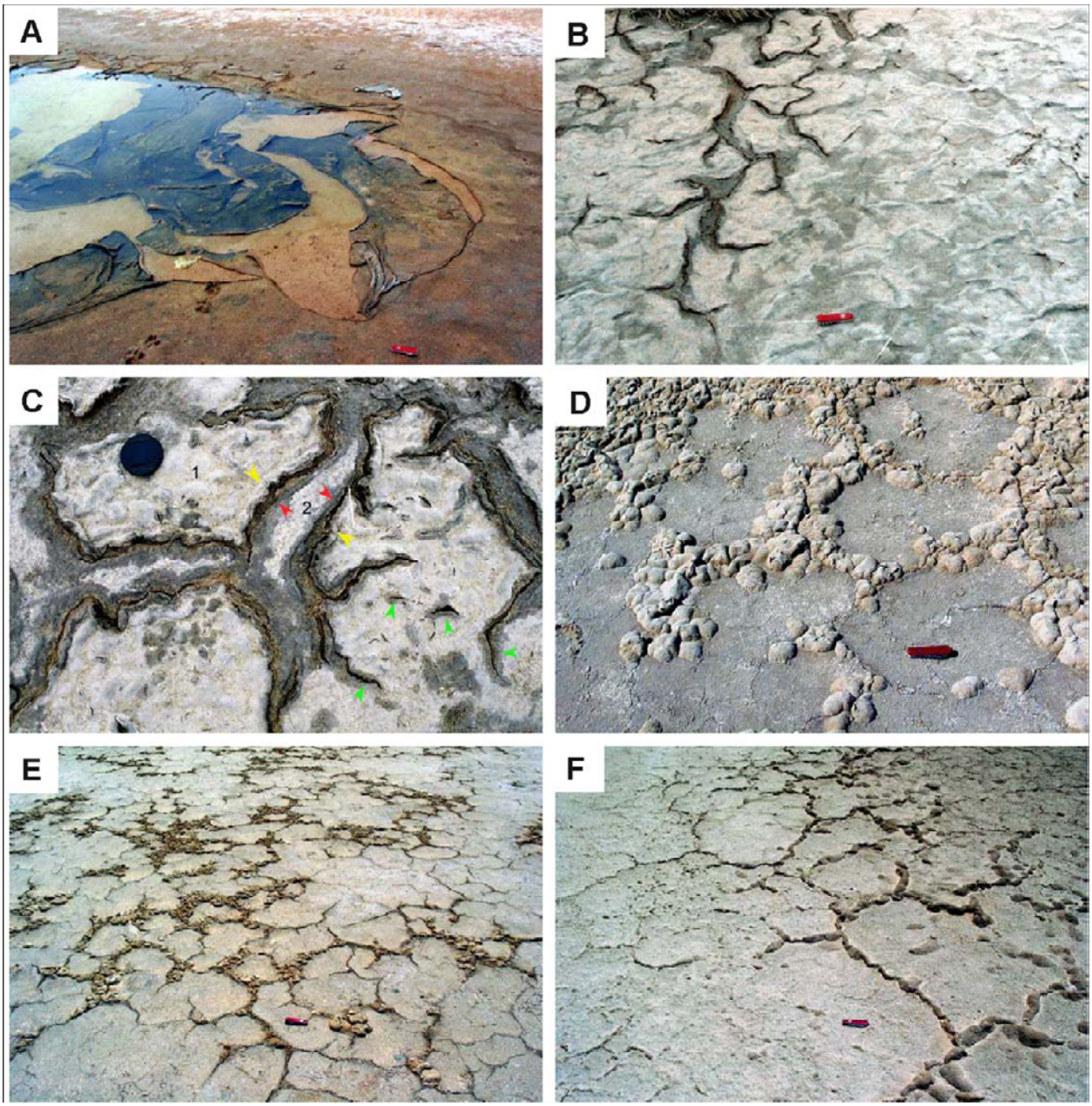

In: *Atlas of microbial mat features preserved within the clastic rock record,* Schieber, J., Bose, P.K., Eriksson, P.G., Banerjee, S., Sarkar, S., Altermann, W., and Catuneau, O., (Eds.)J. Schieber et al. (Eds.), Elsevier, p. 258-265. (2007)

Figure 8(d)-2: Possible implications of elevated seepage pressure in confined sediment underneathmicrobial mat.
(A) Detached and floating mat in supratidal pond. Mat detachment and outflow of groundwater is interpreted here as 'floating failure' due to groundwater recharge after heavy rainfall in the hinterland. Mat detachment and flotation may, however, also have resulted from excessive photosynthetic gas production or may have occurred after flooding of a desiccated mat. Sabkha El Grine, southern Tunisia. Scale (knife) is 8 cm. (B) Strongly cohesive microbial mat with 'leaking' shrinkage cracks. Cracks and crack margins are overgrown by new microbial layers due to availability of water rising up from below. Sabkha Jellabia, southern Tunisia. Scale (knife) is 8 cm. (C) Details of shrinkage, 'leaking cracks' and microbial overgrowth in subaerially exposed mat. Old mat (1) with first generation cracks (yellow arrows) overgrown by younger mat (2) undergoing renewed cracking (red arrows). Dark zones along new cracks indicate elevated humidity and microbial activity. Green arrows show new cracks accompanied by increased microbial activity in old mat. Sabkha Jellabia, southern Tunisia. Scale (lens hood) is 6 cm. (D) Structures resulting from localised microbial growth along narrow shrinkage cracks in flat mat. Doming supported by a *Microcoleus* mat, irregular shape of these growth-induced 'mat expansion structures' ('petees') suggests preferential activity of coccoid bacteria. Upper intertidal to lower supratidal zone, Sabkha Bou Jemel, southern Tunisia. Scale (knife) is 8 cm. (E) Domal 'mat expansion structures' resulting from localised microbial growth along polygonally arranged shrinkage cracks. Groundwater discharge at crack openings is considered responsible for local growth activity. Upper intertidal to lower supratidal zone, Sabkha Bou Jemel, southern Tunisia. Scale (knife) is 8 cm. (F) Round-crested bulges following trends of polygonal shrinkage cracks. The bulges are interpreted as 'mat expansion structures' resulting from localised microbial growth along 'leaking cracks'. Desiccated, shallow, supratidal pond, Sabkha Bou Jemel, southern Tunisia. Scale (knife) is 8 cm.

In: *Atlas of microbial mat features preserved within the clastic rock record,* Schieber, J., Bose, P.K., Eriksson, P.G., Banerjee, S., Sarkar, S., Altermann, W., and Catuneau, O., (Eds.)J. Schieber et al. (Eds.), Elsevier, p. 258-265. (2007)

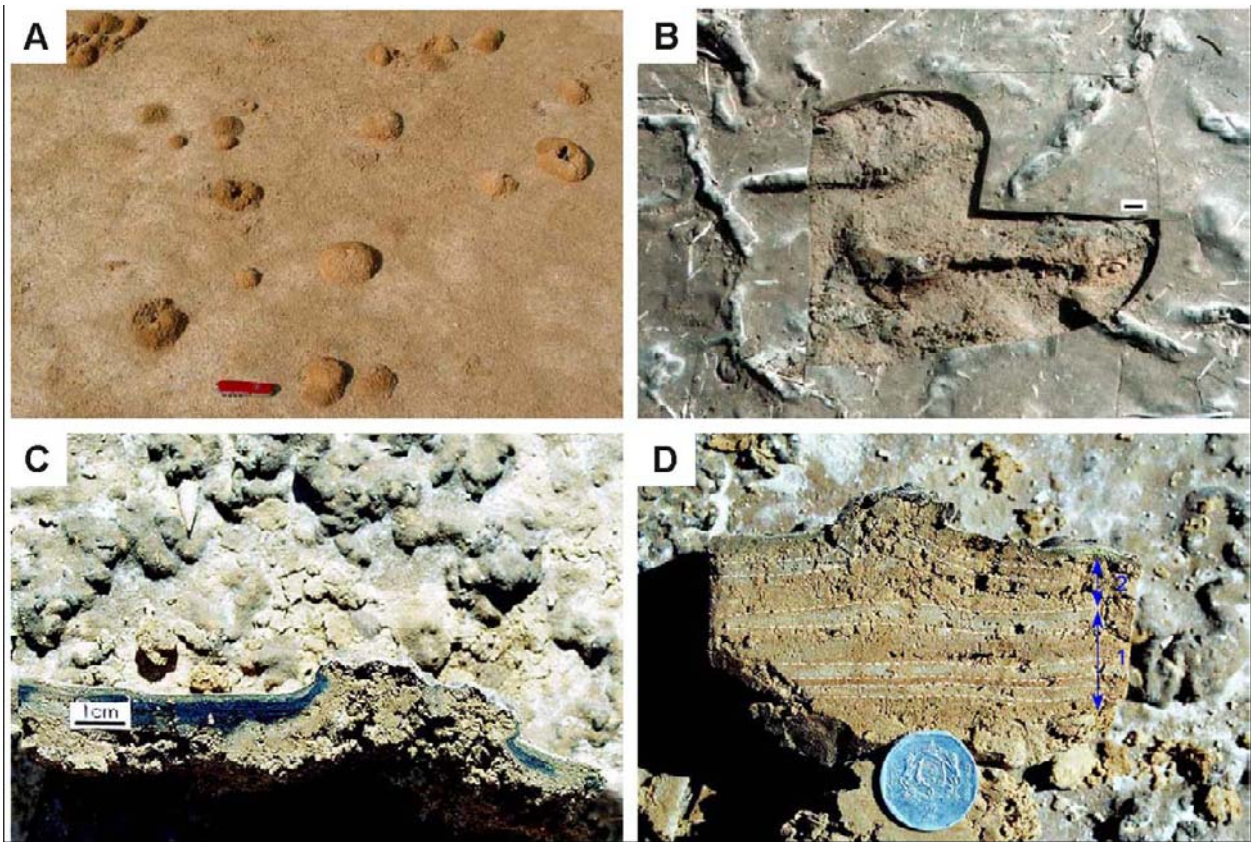

Figure 8(d)-3: Possible implications of seepage pressure and a potential for liquefaction in confined sediment underneath microbial mat.
(A) Isolated domal structures developed on thin, gypsum-encrusted microbial mat of mainly coccoid cyanobacteria. The domes have formed above vertical burrows of rove beetles (*Bledius* sp.). The burrows provided pathways for seepage of groundwater triggering local microbial growth and precipitation of gypsum. Supratidal zone, Sabkha Bou Jemel, southern Tunisia. Scale (knife) is 8 cm. (B) Microbial mat with linear and irregular bulges, filled from below by ascending sediment of the mat substratum. Scale is 2 cm. Bhar Alouane tidal flat, southern Tunisia. (C) Section across 'pustular', *Synechococcus*-type mat showing surface irregularities filled from below by rising sediment. Surface features of the mat are seen in background (upper part of photograph). Sabkha El Mdeina, southern Tunisia. (D) Section across microbial mat with bulge filled by sediment rising up from the mat substratum. Dashed lines indicate layers of undisturbed bedding (1) overlain by disturbed layers in the top 15–20 mm (2). Supratidal zone, Sabkha El Grine, southern Tunisia. Scale (coin) is 24 mm.

In: *Atlas of microbial mat features preserved within the clastic rock record,* Schieber, J., Bose, P.K., Eriksson, P.G., Banerjee, S., Sarkar, S., Altermann, W., and Catuneau, O., (Eds.)J. Schieber et al. (Eds.), Elsevier, p. 258-265. (2007)

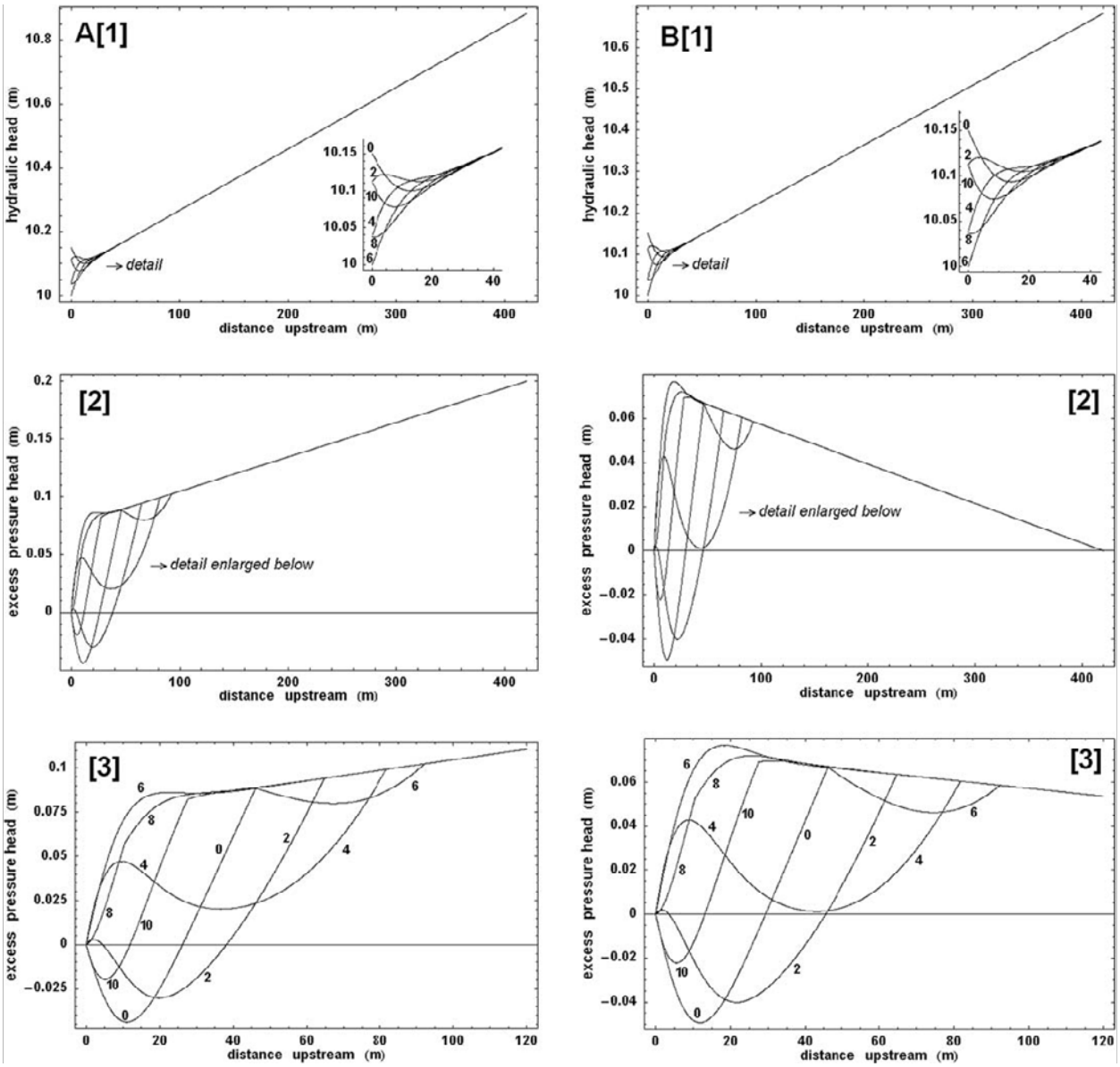

Figure 8(d)-4: Hydraulic head profiles.
Spatial distribution of hydraulic head and of excess pressure head: case A (plots on the left, A) and case B (plots on the right, B). The head profiles ($A_{[1]}$, $B_{[1]}$) are almost identical but the excess pressure head, i.e., the energy available for liquefaction ($A_{[2]}$, $B_{[2]}$) is lower in case B, and generally decreases with the distance from the sand barrier, vanishing in the vicinity of the pond.Within some 90 m from the sand barrier, the thickness of the liquefied layer oscillates in both cases, experiencing periodic 'freezing'; beyond about 90 m distance from the sand barrier, the liquefied thickness no longer varies with time (tide influence is no longer felt). Labels "0", "2", . . . , "10" on the zoom-in plots ($A_{[3]}$, $B_{[3]}$) indicate hours elapsed from high-tide. Simulation parameters: aquifer length: 420 m, geodetic slope: 1/615, hydraulic conductivity: 10^{-5} m/s, aquifer thickness: 10 m, storativity: 2×10^{-2} (or 2×10^{-3} m^{-1}), maximum tide height: 15 cm, water level in pond: 20 cm (case A), 0 (case B).

In: *Atlas of microbial mat features preserved within the clastic rock record,* Schieber, J., Bose, P.K., Eriksson, P.G., Banerjee, S., Sarkar, S., Altermann, W., and Catuneau, O., (Eds.)J. Schieber et al. (Eds.), Elsevier, p. 258-265. (2007)

References

Black, M. (1933). The algal sediments of Andros Islands, Bahamas. Phil. Trans. Royal Soc. London, Ser. B: 165-192.

Butler, G. (1969). Modern evaporite deposition and geochemistry of coexisting brines. The Sabkha, Trucial Coast, Arabian Gulf: Journal of Sedimentary Petrology, 39, 70-89

Cameron, B., Cameron, D. and Richard J. (1985). Modern algal mats in intertidal and supratidal quartz sands, northeastern Massachusetts, U.S.A. In: Biogenic Structures: their Use in Interpreting Depositional Environments (Ed. H.A. Curran), SEPM Spec. Publ., 35, 211-223.

Decho, A.W., (1994). Molecular-scale events influencing the macroscale cohesiveness of exopolymers. In: Krumbein, W.E., Paterson, D.M. and Stal, L.J. (Eds), Biostabilization of Sediments. BIS Verlag, Oldenburg, pp. 134-148.

Fenchel, T. and Kühl, M (2000). Artificial cyanobacterial mats: growth, structure, and vertical zonation patterns. Microb. Ecol., 40, 85-93; DOI: 10.1007/s002480000062.

Gerdes, G., Krumbein, W.E., Reineck, H.E. (1985). Verbreitung und aktuogeologische Bedeutung mariner mikrobieller Matten im Gezeitenbereich der Nordsee. Facies, 12, 75-96.

Gerdes, G., Klenke, Th., Noffke, N. (2000). Microbial signatures in peritidal siliciclastic sediments: a catalogue. Sedimentology, 47, 279-308.

Hsü, K., and Siegenthaler, C. (1969). Preliminary experiments on hydrodynamic movement induced by evaporation and their bearing on the dolomite problem: Sedimentology, 12, p. 11–25.

Kendall, C.G.ST.C. and Skipwith, P.A.d'E. (1969). Geomorphology of a recent shallow-water carbonate province: Khor Al Bazam, Trucial Coast, Southwest Persian Gulf. Geol. Soc. Am. Bull., 80, 865-891

Kinsman, D.J.J. and Park, R.K. (1976). Algal belt and coastal sabkha evolution, Trucial Coast, Persian Gulf. In: Stromatolites, (Ed. R.M. Walter), Dev. Sedimentol., 20, 421-433.

Noffke, N. (1998) Environmental requirements for microbial mat formation in Recent tidal systems. Abstracts, Sediment '98, 9-13. 6. 1998, Erlangen.

Noffke, N., Gerdes, G., Klenke, T., Krumbein, W.E. (1996). Microbially induced sedimentary structures – examples from modern sediments of siliciclastic tidal flats. Zentralbl. Geol. Paläontol. I, 1995 (1/2), 307-316.

Noffke, N., Gerdes, G., Klenke, T., Krumbein, W. (2001a). Microbially induced sedimentary structures indicating climatological, hydrological and depositional conditions within Recent and Pleistocene coastal facies zones (Southern Tunesia). Facies, 44, 23-30.

Noffke, N., Gerdes, G., Klenke, T., Krumbein, W.E. (2001b) Microbially induced sedimentary structures – a new category within the classification of primary sedimentary structures. J. Sed. Res., 71, 649-656.

Noffke, N., Gerdes, G. and Klenke, T. (2003). Benthic cyanobacteria and their influence on the sedimentary dynamics of peritidal depositional systems (siliciclastic, evaporitic salty, and evaporitic carbonatic). Earth-Sci. Rev., 62, 163-176.

Reineck, H.E. (1979). Rezente und fossile Algenmatten und Wurzelhorizonte. Natur u. Museum 109, 290-296.

Reineck, H.-E., Gerdes, G., Claes, M., Dunajtschik, K., Riege, H. and Krumbein, W.E. (1990) Microbial modification of sedimentary surface structures. In: Sediments and Environmental

Geochemistry, (Eds. D. Heling, P. Rothe, U. Förstner and P. Stoffers), pp. 254-276. Springer-Verlag, Berlin.
Stal, L.J. (2000). Cyanobacterial mats and stromatolites. In: Whitton, B.A. and Potts, M. (Eds.), The ecology of cyanobacteria. Kluwer Academic Publishers, pp. 61-120.
Watson, I, and Burnett, A.D. (1995). Hydrogeology. An environmental approach: CRC Press, Boca Raton, London, Tokyo, 702 pp.
Zavarzin, G.A. (2003). Diversity of cyano-bacterial mats. In: Krumbein, W.E., Paterson, G.A. and Zavarzin, G.A. (eds): Fossil and Recent Biofilms. Kluwer Academic Publishers, Dordrecht, pp. 141-150.

Appendix 1

Modelling hydraulic conditions in a sediment layer confined beneath a microbial mat

As previously described in the text, upwardly directed 'hydraulic pressure' (seepage pressure) is implicit when water completely filling the pore space is flowing downslope through a confined aquifer. In the following modelling, the tide-modulated distribution of this pressure will be calculated. Additionally, the question is posed whether, and under which conditions, 'hydraulic pressure' may attain values sufficient for liquefaction. This is of particular interest as potential for liquefaction would allow grain displacement and structural changes in the sediment underneath microbial mats.

Boundary conditions

Boundary conditions for hydraulic modelling (Fig. 8(d)-4) are based on data derived from the natural example described above in the text. Conditions embrace a low-gradient, seaward sloping flat sediment surface that is continuously covered by a quasi-impermeable surface layer. The sediment confined beneath the sealing surface layer is water-saturated and, following the 'flood water recharge model' of Butler (1969), a steady or periodic downslope groundwater flow from the hinterland or from supratidal ponds that were filled with water during spring tides, storms or rainfalls is assumed. The grain size of the sediment is in the range of fine-grained sand. Tidal waters encroach upon the surface, up to a distance of 100 m from the sea, at high tides.

Modelling hydraulic conditions in the confined layer

In the following, it will be shown how tide-modulated seepage pressure distribution is computed for a gently-sloping confined aquifer, and how conditions for liquefaction of an unconsolidated sand layer at the aquifer-top can be derived. Two cases will be considered: Case A is a time when the groundwater flow is still strong, visualized by a completely filled supratidal pond. Case B is a later point of time when the groundwater flow is waning to almost ceasing, but traces of water are still present (the pond is close to drying out).

For a loosely-granular aquifer layer, a criterion for liquefaction onset can be formulated in terms of the weight of an individual grain to be displaced locally by virtue of seepage pressure, whereas for liquefaction across a finite layer thickness a condition can be formulated in terms of the weight of the corresponding grain-filled column to be displaced by the action of seepage pressure over a finite height. Denoted by $h = h(x,z)$, the hydraulic head driving water flow ($v = K \cdot \nabla h$) in the aquifer (treated as two-dimensional, with geodetic height z and longitudinal coordinate x), the seepage pressure at point (x,z) is $P(x,z) = \rho_w g(h(x,z) - z)$ and it will exceed the weight pressure of a single grain if $h(x,z) - z > \rho_g d_g / (n_0 \rho_w)$, in which n_0 denotes the undisturbed (initial) porosity, d_g a characteristic grain size, ρ_g the bulk grain density and ρ_w water density. By this criterion, very little seepage pressure (just a few millimetres) would be sufficient to lift a single grain against its own gravity, were there no further cohesion or confining

In: *Atlas of microbial mat features preserved within the clastic rock record,* Schieber, J., Bose, P.K., Eriksson, P.G., Banerjee, S., Sarkar, S., Altermann, W., and Catuneau, O., (Eds.)J. Schieber et al. (Eds.), Elsevier, p. 258-265. (2007)

(downward) forces, including the weight of the material column on top of the grain. For seepage pressure to displace against gravity a whole grain-filled column of undisturbed porosity n_0 and thickness δ_{liq} (neglecting any cementation, cohesion and contact forces), the seepage pressure head $h(x,z) - z$ must exceed $\delta_{liq}\,\rho_g / \rho_w$, the result being in the range of 3-4 times the thickness δ_{liq} . For instance, to achieve liquefaction across the topmost centimetre of unconsolidated granular aquifer material, the seepage pressure head at the aquifer-top must exceed 3-4 centimetres.

As mentioned before, this criterion relies on the idealised assumption that there are no further confining (downward) forces acting on the grain layer at the aquifer-top. In reality, the aquifer will either be confined, which means additional downward forces acting on the material at the aquifer-top, or it will have a phreatic surface at which $h(x,z) - z \rightarrow 0$. So, the liquefaction criterion formulated in terms of 'material column weights' will only find its application in certain exceptional situations in which, for instance, the aquifer may be treated as confined, as regards the hydraulic flow field, but the confining force on the aquifer-top may be considered as negligible, as regards force balances. One such exceptional situation is that of a shallow aquifer under direct tidal influence and 'confined' by a thin microbial mat as described before.

The time-periodical distribution of seepage pressure head $p(x,z,t) \rightarrow p(x,t)$ at the aquifer-top is computed for peritidal conditions in the sandy aquifer under the following simplifying assumptions:

(1) The aquifer-base is horizontal ($z = 0$), the aquifer-top $z(x) = B + \gamma x$ is gently sloping with constant geodetic slope $\gamma<<1$, thus the aquifer extends from $x = 0$ to $x = L$ with approximately constant thickness (B) and transmissivity ($k_f B$). At $x = 0$ the aquifer is in direct contact with the sea water surface; at $x = L$ there is a supratidal pond, in which the water level may vary between 0 and H_{max}, but may be treated as approximately constant over a short succession of tidal events (say, a couple of days).

(2) The Dupuits assumption applies: $\partial_z h << \partial_x h$, the head distribution can be approximated as 1D: $h(x,z,t) \rightarrow h(x,t)$.

(3) Apart from liquefaction within a very thin layer at the aquifer-top, material aquifer properties do not vary in space and time; hydraulic diffusivity (transmissivity/storativity) $k_f B / S$ maintains the same value throughout.

(4) The sand material under the mat is fully water-saturated at all times, and mat elasticity (deformation) has negligible impact upon storage in the aquifer, thus the aquifer may be treated as fully confined.

(5) Direct recharge/infiltration through the microbial mat is negligible; driving forces for flow in the aquifer (which may change direction) are provided by tidal height as well as by the water level in the supratidal pond at the other end and, of course, gravity itself throughout the

aquifer. Consistently with the Dupuits assumption, the aquifer boundaries at $x = 0$ and $x = L$ enjoy full hydraulic contact over the whole aquifer depth.

At the aquifer-top, the excess pressure $p^*(x,t)$ (i.e., the part of seepage pressure actually available for liquefaction), is what remains from seepage pressure $p(x,t)$ after subtracting the confining (downward) force acting on the grains at aquifer-top, assumed to consist only of the weight of the water column above the mat (mat thickness being negligible, and mat substance not being essentially heavier than water). The height of the water column varies in time, but is assumed to be determined only by the advancing or regressing tidal water-front. Solving the boundary-value problem for $p(x,t)$ with a time-periodic boundary condition at $x = 0$, yields the following closed form for $p^*(x,t)$:

$$
\begin{aligned}
& H_{\mathsf{T}} + \left(\frac{H_{\mathsf{P}} - H_{\mathsf{T}}}{L} + \frac{q_{\mathsf{R}} L}{2a}\right) x - \frac{q_{\mathsf{R}}}{2a} x^2 + \\
& + \frac{H_{\mathsf{T}}}{2} \frac{e^{k\tilde{x}} \cos(\omega t - kx) + e^{-k\tilde{x}} \cos(\omega t + kx) - e^{kx} \cos[\omega t - k\tilde{x}] - e^{-kx} \cos[\omega t + k\tilde{x}]}{\cosh(2kL) - \cos(2kL)} \\
& \underbrace{- \frac{1}{2} \left\{ \left| \gamma x - H_{\mathsf{T}} \left[1 + \cos\left(\omega t - \pi \frac{\gamma x}{2H_{\mathsf{T}}}\right)\right] \right| + \gamma x - H_{\mathsf{T}} \left[1 + \cos\left(\omega t - \pi \frac{\gamma x}{2H_{\mathsf{T}}}\right)\right] \right\}} \\
& = \begin{cases} 0 & \text{if } x \leqslant \frac{H_{\mathsf{T}}}{\gamma} \left[1 + \cos\left(\omega t - \pi \frac{\gamma x}{2H_{\mathsf{T}}}\right)\right] \\ \gamma x - H_{\mathsf{T}} \left[1 + \cos\left(\omega t - \pi \frac{\gamma x}{2H_{\mathsf{T}}}\right)\right] & \text{if } x > \frac{H_{\mathsf{T}}}{\gamma} \left[1 + \cos\left(\omega t - \pi \frac{\gamma x}{2H_{\mathsf{T}}}\right)\right] \end{cases}
\end{aligned}
$$

incorporating the effect of following factors:

notation	meaning	dimension	value used to produce the plots (Fig. 8(d)-2)
H_T	tide amplitude (half of max. tide level)	*Length*	7.5 cm
H_P	thickness of water layer in pond (pond water level, relative to pond-bottom)	*Length*	20 cm (case A) 0 (case B)
L	aquifer length	*Length*	420 m
γ	geodetic slope (assumed as uniform)	1	1 / 615
a	hydraulic diffusivity (aquifer transmissivity/storativity)	$length^2/time$	432 m^2/day
ω	tide (angular) frequency	$time^{-1}$	$2\pi \times (12 \text{ hours})^{-1}$ =

			12.6 day^{-1}
k	coupling parameter (tides – hydraulics), defined as $k = \omega^{1/2} (2a)^{-1/2}$	*length*$^{-1}$	0.121 m^{-1}
q_R	surface recharge through mat	*length/time*	neglected as it has no influence upon time-varying terms
T	time variable	*Time*	(variable)
x	space variable (distance from barrier; $x = 0$ at barrier; $x = L$ at upslope pond)	*length*	(variable)
$\widetilde{x}$	reflected space variable, defined as $2L - x$	*Length*	(variable)

Interpretation

Depending on the aquifer parameters and the relative tide vs. pond heights, there will exist a region between $x = 0$ and $x = L$ in which sand liquefaction underneath the mat appears possible at all times. For the examples shown in Fig. 8(d)-4A, -4B this will be the case at distances exceeding ca. 40 m and ca. 50 m from the sand barrier, respectively. Below these distances are complementary regions in which sand liquefaction underneath the mat appears possible only for a certain number of hours every day. Also, the depth of the (potentially) liquefied layer δ_{liq} varies with the distance from the barrier and, additionally, with the tides (variations remaining strictly periodic as long as no macroscopic change of the system or material hysterese effects become noticeable). Thus, within ca. 90 m from the barrier, the liquefied layer oscillates in thickness between +0 cm and about 3 cm and will experience periodic ‘freezing’, i.e. compression around high tides, due to the load of overlying tidal water. Close to the barrier, the direction of flow within the sand layer will periodically revert from prevailing downslope to an upslope direction, for about 6 hours every tide period (±3 hours from high tide).

As may be inferred from Fig. 8(d)-4$A_{[1]}$ and $B_{[1]}$, the direction of flow within the sand layer periodically reverts from prevailing downslope to upslope direction, close to the barrier. Thus, at about 40 m distance from the sand barrier a local, minor ‘groundwater divide’ will exist for about 6 hours every tide period (± 3 hours from high tide).